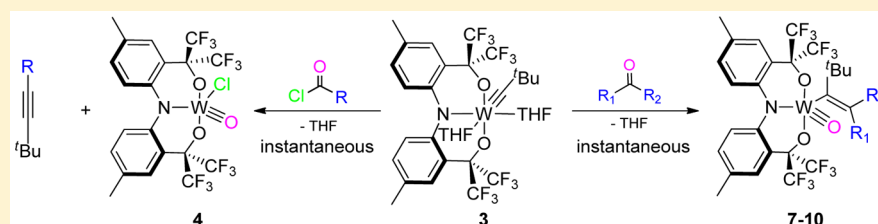


Fast “Wittig-Like” Reactions As a Consequence of the Inorganic Enamine Effect

Stella A. Gonsales, Matias E. Pascualini, Ion Ghiviriga, Khalil A. Abboud, and Adam S. Veige*

Department of Chemistry, Center for Catalysis, University of Florida, P.O. Box 117200, Gainesville, Florida 32611, United States

S Supporting Information



ABSTRACT: The tungsten alkydine $[\text{CF}_3\text{-ONO}]\text{W}\equiv\text{CC}(\text{CH}_3)_3(\text{THF})_2$ (**3**) {where $\text{CF}_3\text{-ONO} = (\text{MeC}_6\text{H}_3[\text{C}(\text{CF}_3)_2\text{O}])_2\text{N}^{3-}$ } supported by a trianionic pincer-type ligand demonstrates enhanced nucleophilicity in unusually fast “Wittig-like” reactions. Experiments are designed to provide support for an inorganic enamine effect that is the origin of the enhanced nucleophilicity. Treating complex **3** with various carbonyl-containing substrates provides tungsten-oxo-vinyl complexes upon oxygen atom transfer. The rates of reactivity of **3** are compared with the known alkydine $(\text{DIPP})_3\text{W}\equiv\text{CC}(\text{CH}_3)_3$ (DIPP = 2,6-diisopropylphenoxide). In all cases (except acetone), complex **3** exhibits significantly faster overall rates than $(\text{DIPP})_3\text{W}\equiv\text{CC}(\text{CH}_3)_3$. New oxo-vinyl complexes are characterized by NMR, combustion analysis and single crystal X-ray diffraction. Treating **3** with acid chlorides provides the tungsten oxo chloride species $[\text{CF}_3\text{-ONO}]\text{W}(\text{O})\text{Cl}$ (**4**) and disubstituted alkynes. In the case of acetone the oxo-vinyl complex results in two rotational isomers **10_{syn}** and **10_{anti}**. The rate of isomerization was determined for the forward and reverse directions and was complimented with DFT calculations.

INTRODUCTION

Creating highly nucleophilic metal–carbon multiple bonds is an important synthetic challenge and can result in new and unusual reactivity. For example, the trianionic ONO^{3-} pincer alkydine $[\text{CF}_3\text{-ONO}]\text{W}=\text{CHCH}_2\text{CH}_3(\text{O}^t\text{Bu})$ deprotonates its own *tert*-butoxide ancillary ligand to release isobutylene producing the tungsten oxo-alkyl complex $[\text{CF}_3\text{-ONO}]\text{W}(\text{O})\text{CH}_2\text{CH}_2\text{CH}_3$.¹ From Mindiola’s laboratories, the pincer supported titanium alkydine $[(\text{PNP})\text{Ti}\equiv\text{CC}(\text{CH}_3)_3]^{2-4}$ (where $\text{PNP}^- = \text{N}[2\text{-P}^i\text{Pr}_2\text{-4-methylphenyl}]_2$) can activate C–H bonds from benzene, methane, ethane, propane, linear alkanes C4–C8, and some cyclic alkanes.^{5–7} A method to elevate the nucleophilicity of metal–carbon multiple bonds is to apply the “inorganic enamine” effect.¹ Figure 1 depicts the relationship between organic enamines⁸ and an inorganic enamine via a straightforward resonance depiction. Constraining an N atom lone pair to be collinear with a metal–carbon multiple bond is the basis for the interaction. In both cases, the resonance contributions effectively delocalize the N atom lone

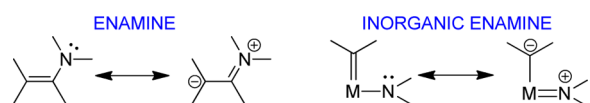


Figure 1. Resonance contributions for an enamine (left) and the analogous inorganic enamine (right).

pair electron density across the unsaturated bond to the carbon two bonds away.

Figure 2 depicts a truncated molecular orbital diagram that summarizes previous work on the electronic consequences of the inorganic enamine effect.¹ In Figure 2A, the amido ligand rotates freely, thus the lone pair on nitrogen preferentially orients to maximize overlap with the empty d_{xy} orbital on the metal. The interaction stabilizes the N atom lone pair in a bonding molecular orbital as the HOMO. It is clear that no electron density resides on the α -carbon of the alkydine. In contrast, a trianionic ONO^{3-} pincer ligand constrains the N atom lone pair in Figure 2B to be coplanar with one of the metal–carbon π -bonds. The forced interaction has three important effects: (1) the interaction splits the energies of M–C π -bonding orbitals; (2) the HOMO orbital is π^* in character, and thus overall is destabilized; and (3) the HOMO orbital contains significant electron density on the α -carbon, akin to an enamine. Taken together the inorganic enamine effect destabilizes the complex and accentuates the nucleophilicity of the α -carbon.

Positive support that the inorganic enamine effect is indeed real requires the α -carbon to not only react with protons, but other electrophiles as well, and the reactivity should be accelerated, i.e., demonstrably more nucleophilic. Herein, we

Received: February 12, 2015

Published: March 20, 2015

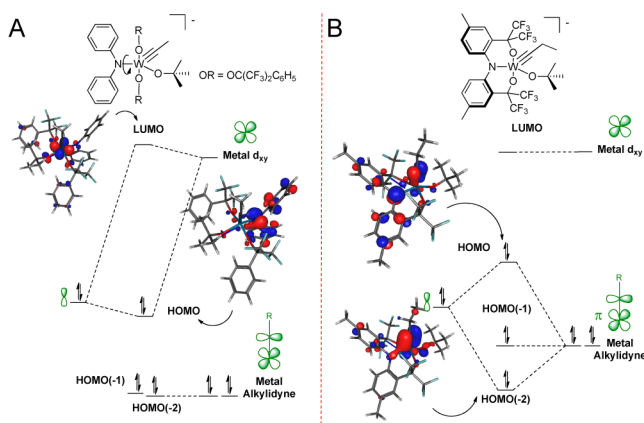


Figure 2. Truncated molecular orbital diagram illustrating the electronic consequences of an inorganic enamine. (A) Amido ligand freely rotates and preferentially orients to overlap with the N atom lone pair with the unoccupied d_{xy} orbital and (B) constrained within a pincer ligand the N atom lone pair is forced to overlap with one of the W–C π -bonds.¹

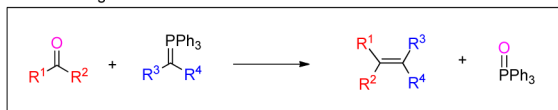
present extraordinarily rapid Wittig-like reactions with the trianionic pincer alkyldiyne complex $[\text{CF}_3\text{-ONO}]\text{W}\equiv\text{CC}(\text{CH}_3)_3(\text{THF})_2$. A combined, synthetic, kinetic, and theoretical analysis provides conclusive evidence for the accentuated nucleophilicity of metal–carbon multiple bonds within an inorganic enamine.

RESULTS AND DISCUSSION

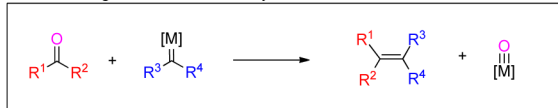
Predicting chemical outcomes based solely on the electronic structure of molecules is critical to discovering new reactivity. A classic case is the juxtaposition of Schrock alkydienes/ynes^{9,10} and Fischer carbenes/ynes.¹¹ As predicted by their electronic structure, high-oxidation-state metal carbon multiple bonds are nucleophilic and exhibit Wittig chemistry (Scheme 1). Tebbe's reagents $\text{Cp}_2\text{Ti}(\mu\text{-CH}_2)(\mu\text{-X})\text{Al}(\text{CH}_3)_2$ ($X = \text{Cl}, \text{Me}$)^{12–15} and Schrock's $(\text{Me}_3\text{CCH}_2)_3\text{M}(\text{=CHCMe}_3)$ ($M = \text{Nb}$ and Ta) alkydienes¹⁶ react with aldehydes, ketones, esters, and amides (Scheme 1B). Alkydienes can also participate in Wittig-like chemistry.^{17,18} $(\text{DIPP})_3\text{W}\equiv\text{CC}(\text{CH}_3)_3$ ($\text{DIPP} = 2,6\text{-diisopro-$

Scheme 1. Wittig and “Wittig-Like” Reactions with Alkydienes and Alkydienes

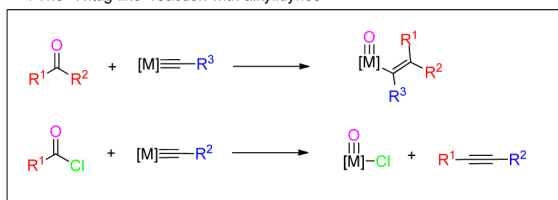
A. The Wittig reaction



B. The “Wittig-like” reaction with alkydienes



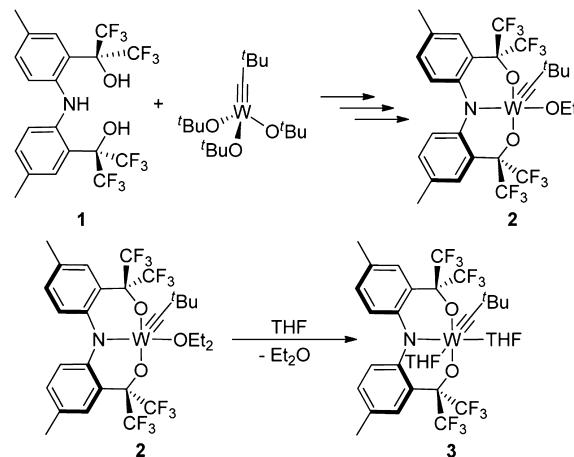
C. The “Wittig-like” reaction with alkydienes



pylphenoxide)¹⁷ cleaves C=O bonds to form oxo-vinyl complexes according to Scheme 1C. In an interesting example, acid chlorides react with $(\text{DIPP})_3\text{W}\equiv\text{CC}(\text{CH}_3)_3$ to produce disubstituted acetylenes in a single step,¹⁸ an overall three bond group transfer. In this work, we use Wittig reactions to evaluate the relative nucleophilicity of metal–carbon multiple bonds.

Reported previously, treating the proligand $[\text{CF}_3\text{-ONO}]\text{H}_3$ (**1**) with $(t\text{BuO})_3\text{W}\equiv\text{CC}(\text{CH}_3)_3$ in Et_2O leads to the trianionic pincer alkyldiyne complex $[\text{CF}_3\text{-ONO}]\text{W}\equiv\text{CC}(\text{CH}_3)_3(\text{Et}_2\text{O})$ (**2**) (Scheme 2).¹⁹ The Et_2O complex can be

Scheme 2. Improved Synthesis of the Tungsten Alkyldiyne $[\text{CF}_3\text{-ONO}]\text{W}\equiv\text{CC}(\text{CH}_3)_3(\text{THF})_2$ (**3**)

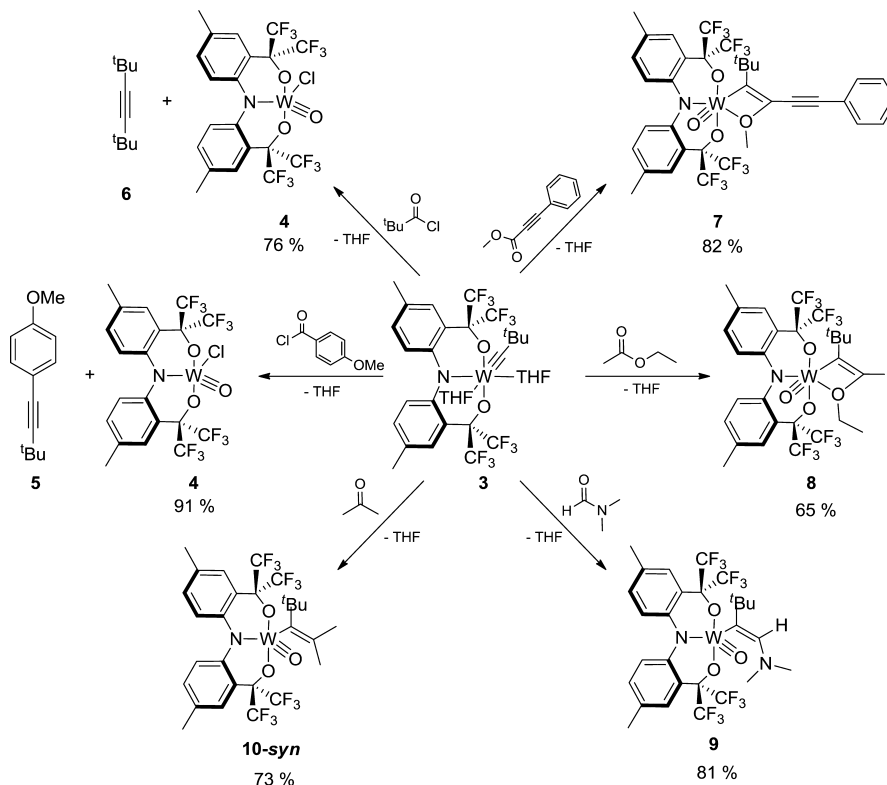


challenging to prepare in pure form. To improve the preparation, treating complex **2** with a few drops of THF produces the bis-THF complex $[\text{CF}_3\text{-ONO}]\text{W}\equiv\text{CC}(\text{CH}_3)_3(\text{THF})_2$ (**3**), which is more amenable to purification and a significant improvement to the synthesis.

Scheme 3 depicts the room-temperature reactivity of complex **3** with various carbonyl-containing substrates. The reaction between **3** and *p*-methoxybenzoyl chloride results in an instantaneous color change from blue to green, to form the oxo-chloride complex $[\text{CF}_3\text{-ONO}]\text{W}(\text{O})\text{Cl}$ (**4**) and 1-(3,3-dimethylbut-1-yn-1-yl)-4-methoxybenzene (**5**), in 91% yield. The net reaction is a peculiar three bond swap, C=O and C–Cl for W=O and W–Cl. The reaction presumably proceeds via first formation of a metallaoxetane^{18,20} followed by β -chloride elimination.²¹ N-atom transfers to acid chlorides proceed via a similar mechanism.^{22,23} Complete conversion and confirmation of the identity of the alkyne was confirmed by ¹H and ¹³C{¹H} NMR spectroscopy. Complex **3** also reacts with pivaloyl chloride to produce **4** and 2,2,5,5-tetramethylhex-3-yne (**6**) in 76% yield.

Following the same procedure, the reactivity of **3** with esters, ketones, and amides, was also explored (Scheme 3). An instantaneous color change from blue to red occurs upon adding 1 equiv of methyl phenylpropiolate to **3**. The red color signals the production of the oxo-vinyl complex $[\text{CF}_3\text{-ONO}]\text{W}(\text{O})\{\kappa\text{-C-O-(CH}_3)_3\text{CC=C(OCH}_3)(\text{C}\equiv\text{CC}_6\text{H}_5)\}$ (**7**), in 82% yield. Interestingly, the alkyldiyne attacks the carbonyl group of phenylpropiolate rather than the alkyne. Attack at the carbonyl must occur first because attack at the alkyne would form a metallacyclobutadiene complex, which is irreversible.¹⁹ Evidence for the identity of complex **7** comes from a combination of solution phase NMR studies and solid-state structural characterization. The ¹⁹F{¹H} NMR spectrum

Scheme 3. Reactivity of 3 with Various Carbonyl Compounds



of 7 exhibits four quartets at -70.28 , -70.56 , -75.51 , and -75.94 ppm, corresponding to each CF_3 group in a C_1 -symmetric compound. The ^1H NMR spectrum exhibits a singlet at 3.23 ppm attributable to the methyl group and the ^tBu protons resonate at 1.63 ppm.

An X-ray diffraction experiment performed on single crystals of 7 provides its unambiguous assignment (Figure. 3).

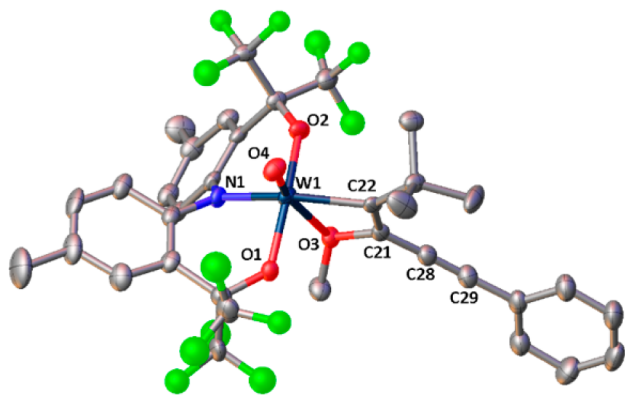


Figure 3. Molecular structure of 7. Ellipsoids are drawn at the 50% probability level, and hydrogen and disordered fluorine atoms are removed for clarity.

Importantly, the molecular structure reveals that the OMe group coordinates to the tungsten ion *trans* to the oxo ligand rendering the complex with a distorted octahedral geometry ($\angle\text{O4-W1-O3} = 163.27(12)^\circ$, $\angle\text{O1-W1-O2} = 159.42(12)^\circ$, and $\angle\text{N1-W1-C22} = 146.04(15)^\circ$). A long W1-O3 bond length of 2.413(3) Å indicates the OMe is weakly bound. For comparison, complex 2 contains a W-OEt₂ bond length that is shorter (2.1144(19) Å).¹⁹ The W1-O4 distance is 1.691(3) Å

and is consistent with related tungsten-oxo complexes.^{23–27} The C28–C29 bond distance is 1.194(6) Å, indicating that the $\text{C}\equiv\text{C}$ triple bond remains intact. A bond length of 1.348(6) Å between C21 and C22 confirms that a newly formed double bond is present in 7.

Complex 3 also reacts immediately in benzene with 1 equiv of ethyl acetate to produce the green oxo-vinyl complex $[\text{CF}_3\text{-ONO}]\text{W}(\text{O})\{\kappa\text{-C-O-(CH}_3\text{)}_3\text{CC}=\text{C}(\text{OCH}_2\text{CH}_3)\text{CH}_3\}$ (8), in 65% yield. ^1H NMR spectroscopic characterization indicates 8 is also C_1 -symmetric and exhibits diastereotopic protons resonating at 3.40 and 3.80 ppm for the $-\text{OCH}_2\text{CH}_3$ protons. The methyl protons ($-\text{OCH}_2\text{CH}_3$) appear as a doublet of doublets centered at 0.33 ppm and the ^tBu protons resonate at 1.43 ppm. Four quartet resonances at -69.74 , -70.59 , -75.12 , and -76.09 ppm in the $^{19}\text{F}\{^1\text{H}\}$ spectrum of 8 offer additional support for a C_1 complex.

Upon treating a benzene solution of 3 with dimethylformamide (DMF), an instantaneous color change from blue to red occurs. Removing the solvent under reduced pressure provides the red oxo-vinyl complex $[\text{CF}_3\text{-ONO}]\text{W}(\text{O})\{(\text{CH}_3\text{)}_3\text{CC}=\text{CH}(\text{N}(\text{CH}_3)_2)\}$ (9) in 81% yield. Crystals suitable for X-ray diffraction deposit from a slowly evaporating solution of 9 in diethyl ether. A combination of ^1H , $^{19}\text{F}\{^1\text{H}\}$, and $^{13}\text{C}\{^1\text{H}\}$ NMR spectroscopy, combustion analysis, and X-ray diffraction studies confirm the identity of 9 (Figure. 4). Clearly different from complex 7, the N atom of the vinyl group in 9 does not coordinate to form a chelate. The metal center adopts a distorted square-pyramidal geometry ($\tau = 0.32$)²⁸ with basal plane angles of $\angle\text{O1-W1-O2} = 156.46(9)^\circ$ and $\angle\text{C21-W1-N1} = 137.13(11)^\circ$. The W1-O3 distance of 1.699(2) Å is statistically identical to 7. Without a chelate such as in 7, the ^tBu group in 9 orients toward open space on the opposite side of the oxo ligand.

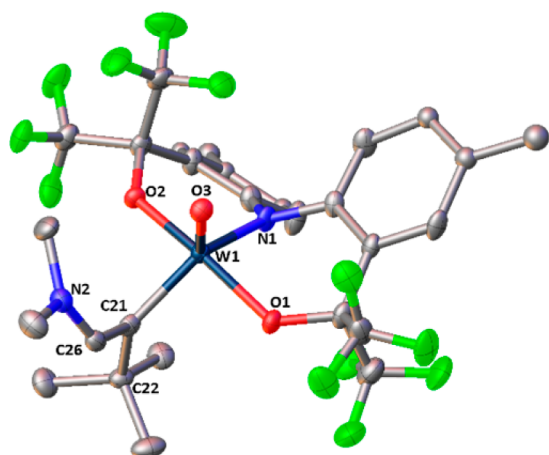
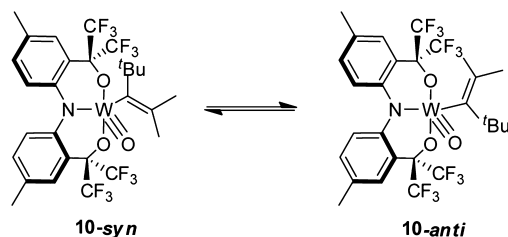


Figure 4. Molecular structure of **9**. Ellipsoids are drawn at the 50% probability level, and hydrogen and disordered arene atoms are removed for clarity.

Complex **3** also deoxygenates acetone to yield the green oxo-vinyl complex $[\text{CF}_3\text{-ONO}]\text{W}(\text{O})\{(\text{CH}_3)_3\text{CC}=\text{C}(\text{CH}_3)_2\}$ (**10**) in 73% yield. Confirmation for the identity of **10** comes from ^1H , $^{19}\text{F}\{^1\text{H}\}$, and $^{13}\text{C}\{^1\text{H}\}$ spectroscopy, elemental analysis, and solid-state characterization. NMR studies indicate that **10** exists as two rotational isomers due to restricted rotation about the W–C bond as **10_{syn}** and **10_{anti}** in a 2:1 ratio (25 °C); where *syn* and *anti* refer to the orientation of the vinyl double bond relative to the oxo ligand (Scheme 4). Similar rotation isomers were assigned to products that form upon reacting $(\text{DIPP})_3\text{W}\equiv\text{CC}(\text{CH}_3)_3$ with acetone, but no X-ray structural data were provided.¹⁷

Scheme 4. Rotational Isomers 10_{syn} and 10_{anti}



Complex **10_{syn}** forms initially as the kinetic product, and then gradual isomerization to **10_{anti}** establishes the equilibrium. The isomerization occurs at room temperature over a period of 20 h and is easily monitored by $^{19}\text{F}\{^1\text{H}\}$ NMR spectroscopy. For the forward reaction of **10_{syn}** to **10_{anti}** a barrier of 23.7 ± 0.4 kcal·mol⁻¹ was determined. In the reverse direction (**10_{anti}** to **10_{syn}**), a barrier of 23.3 ± 0.4 kcal·mol⁻¹ was found. The difference of 0.4 kcal·mol⁻¹ between the two isomers is in agreement with the NMR determined equilibrium distribution of 2:1 for **10_{syn}**:**10_{anti}**.

Insight into the rotation about the W–C bond comes also from DFT calculations at the B3LYP level of theory,^{29–31} where the OWCC dihedral angle was scanned in 10° increments. Figure 5 depicts an asymmetric potential energy surface (PES) as expected for a C₁-symmetric complex. The PES displays two minima corresponding to **10_{syn}** and **10_{anti}** and two high-energy barriers that prevent free rotation about the W–C bond. These barriers result from the large steric hindrance between the flanking CF₃ groups of the pincer and

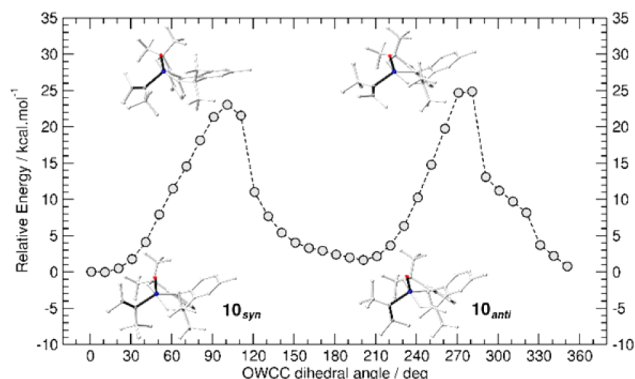


Figure 5. PES scan for the highlighted (black) OWCC dihedral angle of **10**.

the vinyl group. The calculated rotational barriers of 23.04 kcal·mol⁻¹ for the forward reaction and 21.38 kcal·mol⁻¹ for the reverse process are in good agreement with the experimental values.

Green crystals suitable for X-ray diffraction studies grow upon slow diffusion of pentane into a concentrated diethyl ether solution of **10_{syn}** at –23 °C. The solid-state structure (Figure 6) confirms the *syn* orientation. Redissolving the

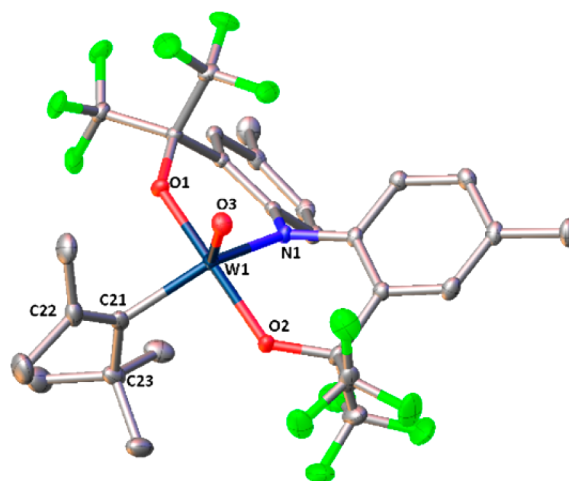


Figure 6. Molecular structure of **10_{syn}**. Ellipsoids are drawn at the 50% probability level, and hydrogen atoms are removed for clarity.

crystals in C₆D₆ and obtaining a ^1H NMR spectrum reveals only resonances attributable to **10_{syn}**, though as before **10_{anti}** slowly forms to establish equilibrium once dissolved. The crystallographic data indicate the tungsten ion adopts a distorted square-pyramidal geometry ($\tau = 0.37$)²⁸ with basal plane angles of $\angle\text{O1-W1-O2} = 159.52(7)^\circ$ and $\angle\text{C21-W1-N1} = 137.46(9)^\circ$. The bond length of 1.365(4) Å between C21 and C22 is appropriate for a C=C double bond, and again the tungsten-oxo bond is similar to **7** and **9** with a bond length of 1.6967(16) Å.

Rates of Reactions: $(\text{DIPP})_3\text{W}\equiv\text{CC}(\text{CH}_3)_3$ vs **3.** Table 1 lists the results from the kinetic analysis for the reaction of various C=O-containing substrates with **3** and $(\text{DIPP})_3\text{W}\equiv\text{CC}(\text{CH}_3)_3$. Impressively, complex **3** exhibits extraordinarily fast overall reaction rates. Schrock reported “Wittig-like” reactivity for the tungsten alkylidyne $(\text{DIPP})_3\text{W}\equiv\text{CC}(\text{CH}_3)_3$,¹⁷ however reaction times of hours were observed for most substrates. For complex **3** each reaction end point occurs within 10 s.

Table 1. Reaction Times and Rates for “Wittig-Like” Reactions Performed with Complexes 3 and (DIPP)₃W≡CC(CH₃)₃

substrate	3		(DIPP) ₃ W≡CC(CH ₃) ₃	
	<i>t</i>	rate ^a M ⁻¹ ·s ⁻¹	<i>t</i>	rate ^a M ⁻¹ ·s ⁻¹
acetone	≤10 s	≥0.002	≤10 s	≥0.002
DMF	≤10 s	≥0.002	12 h ^b	–
EtOAc	≤10 s	≥0.002	2 d	1.2 × 10 ⁻⁷
Ph ₂ CO	≤10 s	≥0.002	90 min	3.7 × 10 ⁻⁶
<i>p</i> -MeOBzCO ₂ Cl	≤10 s	≥0.002	12 h	4.6 × 10 ⁻⁷

^aRate refers to the time frame to complete full conversion.

^bTemperature had to be increased to 50 °C.

Comparing these observations with the ones reported by Schrock,¹⁷ the overall rates for 3 are surprisingly faster (>4 orders of magnitude).

(DIPP)₃W≡CC(CH₃)₃, synthesized according to literature precedent from {(CH₃)₃CH₂}₃W≡CC(CH₃)₃,³² was subjected to the identical reaction conditions as 3. Monitored by ¹H NMR spectroscopy and in sealed NMR tubes, the same concentration of each alkyldiyne was used in all cases (0.02 M in C₆D₆). Complex 3 consumes all substrate within 10 s, thus an estimated minimum overall reaction rate of 0.002 M⁻¹·s⁻¹ for acetone, ethyl acetate, DMF, *p*-methoxybenzoyl chloride, and methyl phenylpropionate was determined. In contrast, changing from brown to deep red, the reaction of (DIPP)₃W≡CC(CH₃)₃ (0.02 M in C₆D₆) with acetone was the only reaction with an instantaneous color change. More typical, adding 1 equiv of ethyl acetate to (DIPP)₃W≡CC(CH₃)₃ results in complete conversion after 2 days. For comparison, complex 3 reacts within 10 s with ethyl acetate with a minimum rate of 0.002 M⁻¹ s⁻¹, whereas (DIPP)₃W≡CC(CH₃)₃ requires 2 days demonstrating a rate of approximately 1.2 × 10⁻⁷ M⁻¹·s⁻¹. The acceleration is 4 orders of magnitude faster for 3. Complex 3 also reacts within 10 s with the larger substrate benzophenone, whereas (DIPP)₃W≡CC(CH₃)₃ requires 90 min. Treating (DIPP)₃W≡CC(CH₃)₃ with DMF instantaneously forms the DMF adduct,¹⁷ however complete conversion to the oxo-vinyl complex requires 12 h heating at 50 °C. For DMF, a direct comparison of reaction rates is not possible since higher temperatures are needed for (DIPP)₃W≡CC(CH₃)₃ to react, but again 3 reacts instantaneously at 25 °C. Formation of acetylene from (DIPP)₃W≡CC(CH₃)₃ and *p*-methoxybenzoyl chloride requires 12 hours to achieve complete conversion resulting in a rate of approximately 4.6 × 10⁻⁷ M⁻¹·s⁻¹, again 4 orders of magnitude slower than 3.

The increased reactivity is not due to the fact 3 contains a trianionic pincer ligand alone. The nitrogen atom in the pincer framework is critical to the inorganic enamine effect. For example, the trianionic OCO³⁻ supported tungsten alkyldiyne complex [tBuOCO]W≡CC(CH₃)₃(THF)₂³³ only binds DMF without further reaction even after heating at 65 °C for 12 h.

CONCLUSION

The trianionic pincer supported complex [CF₃-ONO]W≡CC(CH₃)₃(THF)₂ (3) reacts instantaneously with carbonyl-containing compounds resulting in C=O bond cleavage. The purpose of the study was to establish reactivity rates as a means to support the contention that complex 3 has enhanced nucleophilic character as a consequence of the inorganic enamine effect. A compelling conclusion is possible since

complex 3 reacts up to 4 orders of magnitude faster than (DIPP)₃W≡CC(CH₃)₃. An important result discounts the notion that 3 could be less sterically encumbered than (DIPP)₃W≡CC(CH₃)₃. DMF binds to (DIPP)₃W≡CC(CH₃)₃ instantaneously but takes hours to complete the C=O bond cleavage. The instantaneous binding indicates steric impedance to the metal is not a problem, yet the reaction requires heating to 50 °C for hours to complete. In contrast, complex 3 binds and cleaves the C=O bond in DMF within 10 s. Other Schrock alkyldynes are slow to react; the alkyldiyne (tBuO)₃W≡CC(CH₃)₃ requires 16 h and 60 °C to react with acetone.¹⁷ Combined with the fact that the trianionic OCO³⁻ pincer alkyldiyne complex [tBuOCO]W≡CC(CH₃)₃(THF)₂ does not react with DMF, it is clear that an electronic factor must be responsible for the increased rates observed for 3. The diverse chemistry of metal–carbon multiple bonds is intimately related to the nucleophilicity/electrophilicity of the α-carbon. The “inorganic enamine” effect provides synthetic chemists a new design tool to tailor catalysts.

ASSOCIATED CONTENT

Supporting Information

Full experimental procedures, NMR spectra, and X-ray crystallographic details for CCDC 1048942–1048944. This material is available free of charge via the Internet at <http://pubs.acs.org>.

AUTHOR INFORMATION

Corresponding Author

*veige@chem.ufl.edu

Notes

The authors declare no competing financial interest.

ACKNOWLEDGMENTS

A.S.V. thanks UF and the National Science Foundation for financial support of this project (CHE-1265993). K.A.A. thanks UF and the NSF CHE-0821346 for funding the purchase of X-ray equipment. Computational resources and support were provided by the University of Florida High-Performance Computing Center.

REFERENCES

- O'Reilly, M. E.; Ghiviriga, I.; Abboud, K. A.; Veige, A. S. *J. Am. Chem. Soc.* **2012**, *134*, 11185.
- Bailey, B. C.; Fan, H. J.; Baum, E. W.; Huffman, J. C.; Baik, M. H.; Mindiola, D. J. *J. Am. Chem. Soc.* **2005**, *127*, 16016.
- Mindiola, D. J. *Acc. Chem. Res.* **2006**, *39*, 813.
- Bailey, B. C.; Fan, H. J.; Huffman, J. C.; Baik, M. H.; Mindiola, D. J. *J. Am. Chem. Soc.* **2007**, *129*, 8781.
- Cavaliere, V. N.; Mindiola, D. J. *Chem. Sci.* **2012**, *3*, 3356.
- Cavaliere, V. N.; Crestani, M. G.; Pinter, B.; Pink, M.; Chen, C. H.; Baik, M. H.; Mindiola, D. J. *J. Am. Chem. Soc.* **2011**, *133*, 10700.
- Crestani, M. G.; Hickey, A. K.; Gao, X. F.; Pinter, B.; Cavaliere, V. N.; Ito, J. I.; Chen, C. H.; Mindiola, D. J. *J. Am. Chem. Soc.* **2013**, *135*, 14754.
- Cook, A. G. *Enamines: Synthesis, Structure, And Reactivity*; Marcel Dekker, Inc.: New York, 1988.
- Schrock, R. R. *J. Am. Chem. Soc.* **1974**, *96*, 6796.
- McLain, S. J.; Wood, C. D.; Messerle, L. W.; Schrock, R. R.; Hollander, F. J.; Youngs, W. J.; Churchill, M. R. *J. Am. Chem. Soc.* **1978**, *100*, 5962.
- Fischer, E. O.; Kreis, G.; Kreiter, C. G.; Muller, J.; Huttner, G.; Lorenz, H. *Angew. Chem., Int. Ed. Engl.* **1973**, *12*, 564.

- (12) Tebbe, F. N.; Parshall, G. W.; Reddy, G. S. *J. Am. Chem. Soc.* **1978**, *100*, 3611.
- (13) Scott, J.; Mindiola, D. J. *Dalton Trans.* **2009**, 8463.
- (14) Hartley, R. C.; McKiernan, G. J. *J. Chem. Soc., Perkin Trans. 1* **2002**, 2763.
- (15) Beckhaus, R.; Santamaria, C. J. *Organomet. Chem.* **2001**, *617*, 81.
- (16) Schrock, R. R. *J. Am. Chem. Soc.* **1976**, *98*, 5399.
- (17) Freudenberger, J. H.; Schrock, R. R. *Organometallics* **1986**, *5*, 398.
- (18) Connell, B. T.; Kirkland, T. A.; Grubbs, R. H. *Organometallics* **2005**, *24*, 4684.
- (19) O'Reilly, M. E.; Ghiviriga, I.; Abboud, K. A.; Veige, A. S. *Dalton Transactions* **2013**, *42*, 3326.
- (20) Bazan, G. C.; Schrock, R. R.; Oregan, M. B. *Organometallics* **1991**, *10*, 1062.
- (21) Strazisar, S. A.; Wolczanski, P. T. *J. Am. Chem. Soc.* **2001**, *123*, 4728.
- (22) Sarkar, S.; Abboud, K. A.; Veige, A. S. *J. Am. Chem. Soc.* **2008**, *130*, 16128.
- (23) Clough, C. R.; Greco, J. B.; Figueroa, J. S.; Diaconescu, P. L.; Davis, W. M.; Cummins, C. C. *J. Am. Chem. Soc.* **2004**, *126*, 7742.
- (24) Blosch, L. L.; Abboud, K.; Boncella, J. M. *J. Am. Chem. Soc.* **1991**, *113*, 7066.
- (25) Holm, R. H. *Chem. Rev.* **1987**, *87*, 1401.
- (26) Bonsu, R. O.; Kim, H.; O'Donohue, C.; Korotkov, R. Y.; McClain, K. R.; Abboud, K. A.; Ellsworth, A. A.; Walker, A. V.; Anderson, T. J.; McElwee-White, L. *Dalton Trans.* **2014**, *43*, 9226.
- (27) Chisholm, M. H.; Cook, C. M.; Foltz, K.; Streib, W. E. *Inorg. Chim. Acta* **1992**, *198*, 63.
- (28) Addison, A. W.; Rao, T. N.; Reedijk, J.; Vanrijn, J.; Verschoor, G. C. *J. Chem. Soc., Dalton Trans.* **1984**, 1349.
- (29) Frisch, M. J.; Trucks, G. W.; Schlegel, H. B.; Scuseria, G. E.; Robb, M. A.; Cheeseman, J. R.; Scalmani, G.; Barone, V.; Mennucci, B.; Petersson, G. A.; Nakatsuji, H.; Caricato, M.; Li, X.; Hratchian, H. P.; Izmaylov, A. F.; Bloino, J.; Zheng, G.; Sonnenberg, J. L.; Hada, M.; Ehara, M.; Toyota, K.; Fukuda, R.; Hasegawa, J.; Ishida, M.; Nakajima, T.; Honda, Y.; Kitao, O.; Nakai, H.; Vreven, T.; Montgomery, J. A., Jr.; Peralta, J. E.; Ogliaro, F.; Bearpark, M.; Heyd, J. J.; Brothers, E.; Kudin, K. N.; Staroverov, V. N.; Keith, T.; Kobayashi, R.; Normand, J.; Raghavachari, K.; Rendell, A.; Burant, J. C.; Iyengar, S. S.; Tomasi, J.; Cossi, M.; Rega, N.; Millam, J. M.; Klene, M.; Knox, J. E.; Cross, J. B.; Bakken, V.; Adamo, C.; Jaramillo, J.; Gomperts, R.; Stratmann, R. E.; Yazyev, O.; Austin, A. J.; Cammi, R.; Pomelli, C.; Ochterski, J. W.; Martin, R. L.; Morokuma, K.; Zakrzewski, V. G.; Voth, G. A.; Salvador, P.; Dannenberg, J. J.; Dapprich, S.; Daniels, A. D.; Farkas, Ö.; Foresman, J. B.; Ortiz, J. V.; Cioslowski, J.; Fox, D. J. *Gaussian 09*, revision D.01; Gaussian, Inc.: Wallingford, CT, 2013.
- (30) Becke, A. D. *Chem. Phys.* **1993**, *98*, 5648.
- (31) Lee, C. Y. W.; Parr, R. G. *Phys. Rev. B* **1988**, *37*, 785.
- (32) Churchill, M. R.; Ziller, J. W.; Freudenberger, J. H.; Schrock, R. R. *Organometallics* **1984**, *3*, 1554.
- (33) Sarkar, S.; McGowan, K. P.; Kuppuswamy, S.; Ghiviriga, I.; Abboud, K. A.; Veige, A. S. *J. Am. Chem. Soc.* **2012**, *134*, 4509.